РОССИЙСКАЯ АКАДЕМИЯ НАУК

ЖУРНАЛ
ЭКСПЕРИМЕНТАЛЬНОЙ
И ТЕОРЕТИЧЕСКОЙ ФИЗИКИ

ОСНОВАН В МАРТЕ 1873 ГОДА *ТОМ 114, ВЫПУСК 2(8)*
ВЫХОДИТ 12 РАЗ В ГОД *АВГУСТ , 1998*
МОСКВА «НАУКА»

CONTRIBUTION OF THE MASSIVE PHOTON DECAY CHANNEL TO NEUTRINO COOLING OF NEUTRON STARS

*D. N. Voskresensky**

Moscow Institute for Physics and Engineering
115409, Moscow, Russia
Gesellschaft für Schwerionenforschung
D-64291, Darmstadt, Deutschland

E. E. Kolomeitsev†, *B. Kämpfer*

Institut für Kern und Hadronenphysik, Forschungszentrum Rossendorf
D-01314 Dresden, Deutschland
Institut für Theoretische Physik, TU Dresden D-01062 Dresden, Deutschland

Submitted 15 August 1997

We consider massive photon decay reactions via intermediate states of electron–electron-holes and proton–proton-holes into neutrino–antineutrino pairs in the course of neutron star cooling. These reactions may become operative in hot neutron stars in the region of proton pairing where the photon due to the Higgs–Meissner effect acquires an effective mass m_γ that is small compared to the corresponding plasma frequency. The contribution of these reactions to neutrino emissivity is calculated; it varies with the temperature and the photon mass as $T^{3/2}m_\gamma^{7/2}\exp(-m_\gamma/T)$ for $T < m_\gamma$. Estimates show that these processes appear as extra efficient cooling channels of neutron stars at temperatures $T \simeq 10^9$–10^{10} K.

*E-mail: voskre@rzri6f.gsi.de
†E-mail: kolomei@tpri6f.gsi.de

1. INTRODUCTION

The EINSTEIN, EXOSAT and ROSAT observatories measured surface temperatures of certain neutron stars and put upper limits on the surface temperatures of others (see Ref. [1] and further references therein). Data on the supernova remnants in 3C58, the Crab, and RCW103 indicate rather slow cooling, while the data for Vela, PSR 2334+61, PSR 0656+14, and Geminga point to significantly more rapid cooling. In the so-called standard scenario of neutron star cooling, the most important channel up to temperatures $T \leq 10^8$–10^9 K corresponds to the modified URCA process $n\,n \to n\,p\,e\,\bar{\nu}$. Rough estimates of its emissivity were first made in Ref. [2]. Friman and Maxwell [3] recalculated emissivity of this process in a model, in which the nucleon–nucleon interaction is treated with the help of slightly modified free one-pion exchange. Their result for emissivity, ε_ν^{FM}, proved to be an order of magnitude higher than previously obtained. The value ε_ν^{FM} was used in various computer simulations resulting in the standard cooling scenario; see Ref. [4], for example. Subsequent works [5–7] took in-medium effects into account in NN-interaction, showing that emissivity of the modified URCA process depends heavily on neutron star mass. For stars of more than one solar mass, the resulting emissivities turned out to be substantially higher than the values given by ε_ν^{FM}.

These and other in-medium effects were recently incorporated in the computer code [8] leading to a new scenario of neutron star cooling. For low-mass stars numerical results of the new and standard scenarios more or less coincide. In the present work, we continue to look for enhanced reaction channels. To demonstrate the efficiency of new reaction channels, we compare the results with emissivity ε_ν^{FM}, which dominates cooling in the standard scenario over the temperature range under consideration.

Besides the modified URCA process, the standard scenario numerical codes also include neutron and proton bremsstrahlung processes $n\,n \to n\,n\nu\bar{\nu}$ and $n\,p \to n\,p\nu\bar{\nu}$, which in all models lead to a somewhat smaller contribution to emissivity than the modified URCA process [3, 5, 6, 9]. Also included are processes that contribute to emissivity in the neutron star crust. These are plasmon decay $\gamma_{pl} \to \nu\,\bar{\nu}$ [10, 11], electron bremsstrahlung on nuclei $e\,A \to e\,A\nu\bar{\nu}$ [11–13], electron–positron annihilation $e\,e^+ \to \nu\bar{\nu}$ [14, 15], and photon absorption by electrons $\gamma e \to e\,\nu\bar{\nu}$ [15–17]. Numerical simulations show that the latter two processes contribute only negligibly to the crust neutrino emissivity at the temperatures under discussion in this paper and they always contribute negligibly to the full neutron star's emissivity; see Fig. 7 of Ref. [11].

When the temperature decreases, it is energetically favorable for neutrons to pair in the neutron star interior and inner crust and for the protons to pair in the star's interior. In a system with nucleon pairing the emissivity of the modified URCA process is suppressed by a factor $\exp[-(\Delta_n + \Delta_p)/T]$ [3], where Δ_n and Δ_p are the respective neutron and proton gaps, defined by

$$\Delta_i(T) = \Delta_i(0)\,\frac{T_{c,i} - T}{T_{c,i}}\,\theta(T_{c,i} - T)$$

(here $\theta(x)$ is the Heaviside step function, $i = \{p, n\}$, and $T_{c,i}$ is the corresponding critical temperature for nucleon pairing). At temperatures $T \ll T_{c,p}, T_{c,n}$ the process becomes marginal. Nevertheless, this star's interior process still dominates those of crust cooling up to temperatures $T \sim 10^8$–10^9 K, depending on the values of the gaps; see Fig. 7 of Ref. [11]. For $T \leq (1\text{–}3) \cdot 10^8$ K cooling in the standard scenario is largely dominated by the photon emission from the neutron star surface.

In the present work we look for more efficient cooling processes at $T < T_{c,p}, T_{c,n}$. We analyze photon decay into neutrino–antineutrino pairs. The related processes $\gamma e \to e\,\nu\bar{\nu}$ and $\gamma p \to p\,\nu\bar{\nu}$ turn out to be suppressed by several orders of magnitude compared to those under discussion, due to the lack of free final states in degenerate fermionic systems, and are therefore not considered here. The contribution of photon decay via electron–electron-hole intermediate states for the case of a normal electron plasma in white dwarfs and neutron star crusts has been calculated by several authors (see Ref. [10] for further references). In an ultrarelativistic electron plasma, a photon acquires an effective in-medium plasmon dispersion law with a gap equal to the electron plasma frequency $\omega_{pl} \simeq 2\,e\,\mu_e/\sqrt{3\pi}$, where e is the electron charge and μ_e denotes the electron chemical potential (we employ units with $\hbar = c = 1$). Therefore, the contribution to emissivity of the cited process is suppressed by a factor $\exp(-\omega_{pl}/T)$. Nevertheless, in white dwarfs and neutron star crusts, the electron density is not too high, and the process is still effective. In neutron star interiors, the electron density ρ_e is equal to the proton density ρ_p by virtue electrical neutrality, and along with β stability one obtains a relation for the total density

$$\rho_e = \rho_p \simeq 0.016\,\rho_0 \left(\frac{\rho}{\rho_0}\right)^2, \tag{1}$$

where $\rho_0 \simeq 0.17$ fm^{-3} denotes the nuclear saturation density, and we use the values of the neutron and proton Fermi momenta [3], $p_{Fn} \simeq 340(\rho/\rho_0)^{1/3}$ MeV and $p_{Fp} = \mu_e \simeq$ $\simeq 85(\rho/\rho_0)^{2/3}$ MeV. Thus, at typical densities for neutron star interiors $\rho \gtrsim \rho_0$, the value of the electron plasma frequency is high, e.g., $\omega_{pl}(\rho_0) \approx 4.7$ MeV for $\rho \simeq \rho_0$, and at temperatures $T < T_{c,n}, T_{c,p} < \omega_{pl}$ the process $\gamma_{\omega_{pl}} \to e\,e^{-1} \to \nu\bar{\nu}$, where the superscript -1 denotes the hole, is strongly suppressed. We therefore seek another process that can contribute to rapid cooling.

We exploit the fact that, contrary to a normal electron plasma, in superconducting proton matter, due to the Higgs–Meissner effect, the photon acquires an effective mass that is small compared to the plasmon frequency. In the region of proton pairing at $T < T_{c,p}$, we therefore find that new decay processes of massive photons (γ_m) via electron–electron-hole (ee^{-1}) and proton–proton-hole (pp^{-1}) intermediate states to neutrino–antineutrino pairs, $\gamma_m \to e\,e^{-1} + p\,p^{-1} \to \nu_l\bar{\nu}_l$, $l = \{e, \mu, \tau\}$, can dominate neutron star cooling at certain temperatures. These processes are determined by the diagrams

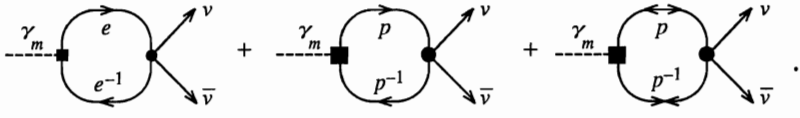

In the first diagram, the solid lines in the loop are related to Green's functions of nonsuperfluid relativistic electrons. In the second and third diagrams, the solid lines in the loops correspond to superconducting nonrelativistic protons. The distinct orientations of arrows indicate that the second diagram is calculated with so-called «normal» Green's functions $\rightarrow\!-$, which become the usual Green's functions for normal Fermi liquids in the limit $\Delta_p \to 0$. In contrast, the third diagram is built up with the «anomalous» Green's functions $\longleftarrow$ and $\rightarrow\!\leftarrow$, which are proportional to the proton gap. Therefore the contribution of the third diagram vanishes for $\Delta_p \to 0$. The fat vertices in the second and third nucleon diagrams include nucleon–nucleon correlations.

The contribution to neutrino production matrix elements of the third diagram and terms proportional to the gap in the second diagram is as small as $(\Delta_p/\epsilon_{Fp})^2 \ll 1$ for $T < T_{c,p} \ll \epsilon_{Fp}$ (here ϵ_{Fp} is the proton Fermi energy), compared to the contribution of the second diagram calculated with the Green's functions of the normal Fermi liquid. To this same accuracy, we drop the third diagram and use the Green's functions of protons for the normal Fermi liquid[1)] in the second diagram. We thus calculate emissivity according to the first two diagrams, assuming $\Delta_p = 0$ in the second diagram but taking into account that the photon dispersion relation is changed due to proton superconductivity.

Our paper is organized as follows. In Sec. 2 we show that in the region of proton superconductivity due to the Higgs–Meissner effect, the photon spectrum is rearranged, and instead of the plasmon gap the photon acquires a mass, which is now determined by the density of paired protons. In Secs. 3 and 4 we demonstrate the efficiency of these new processes in the course of neutron star cooling. The emissivity corresponding to the above diagrams is calculated and compared with emissivity of the standard URCA process and photon emissivity from the neutron star surface. In Sec. 5 we detail our conclusions.

2. PHOTON SPECTRUM IN THE SUPERCONDUCTING PHASE

As is well known [18], the photon spectrum in superconducting matter and in a normal plasma are substantially different. In the superconducting matter considered here, we deal with two subsystems. The normal subsystem contains electrons and nonpaired protons and neutrons, which are present to some extend at finite temperatures. The superfluid subsystem contains paired protons and neutrons. In the presence of a superconducting proton phase, normal currents associated with both electrons and residual nonpaired protons are fully compensated by the corresponding response of the superconducting current [18, 20, 21]; otherwise there would be no superconductivity. What remains after this compensation is a part of the superconducting current. The resulting photon spectrum is thereby determined by the inverse of the London penetration depth (due to the Higgs–Meissner effect [18]), but not by the plasma frequency, as in the normal system.

In convential superconductors, which contain positively charged ions, paired electrons, and normal electrons at $T \neq 0$, the photon spectrum is determined by the relation between the vector potential $\mathbf{A}$ and the current $\mathbf{j}$, which is proportional to $\mathbf{A}$; see Eqs. (96.24) and (97.4) of Ref. [20]. The analogy with the present case is straightforward. From the latter equation, for sufficiently low photon momenta we immediately obtain the relation $4\pi\mathbf{j} \simeq -m_\gamma^2(T)\mathbf{A}$ between the Fourier components of the current and the vector potential, where the effective photon mass is

$$m_\gamma(T) \simeq \sqrt{\frac{4\pi e^2 \rho_p^*(T)}{m_p^*}}, \quad T < T_{c,p}. \tag{2}$$

Here m_p^* denotes the effective in-medium proton mass, and $\rho_p^*(T) = \rho_p(T_{c,p} - T)/T_{c,p}$ denotes the paired proton density. The choice of a linear temperature dependence for ρ_p^* corresponds

[1)] Note that in conventional nuclear physics one usually employs particle–hole diagrams even at zero temperature, thereby considering nuclear matter to be normal. Small effects of pairing can be neglected, since the typical energy in a nucleonic particle–hole diagram is of the order of the Fermi energy ϵ_F, and $\epsilon_F \gg \Delta$ holds [7, 18, 19].

to the Ginzburg–Landau approach. A small complex contribution $\sim e^2 f(\omega, k)\exp(-\Delta_p/T)A_\mu$, where $f(\omega, \mathbf{k})$ is a function of the photon frequency ω and momentum $\mathbf{k}$, has been neglected in the above relation between $\mathbf{j}$ and $\mathbf{A}$. More realistically, for T near $T_{c,p}$, one must take into account this off-shell effect for the photon. At lower temperatures, correction terms are exponentially suppressed. Below we take the photon spectrum to be

$$\omega = \sqrt{\mathbf{k}^2 + m_\gamma^2}, \tag{3}$$

thus neglecting the aforementioned small polarization effects.

Note that external photons cannot penetrate far into the superconducting region. The photons that we deal with are thermal photons with foregoing dispersion law, governed by the corresponding Bose distribution. In considering neutrino reactions below, we integrate over the photon phase-space volume, thus accurately accounting for the distribution of these photons in warm neutron star matter.

To illustrate more transparently the most important facets of the reconstruction of the photon spectrum in the superconducting region, we consider a two-component, locally neutral system consisting of charged fermions (i.e., the normal subsystem) described by the Dirac field ψ, and a charged condensate (i.e., the superconducting subsystem) described by a condensate wave function

$$\varphi = \varphi_c e^{i\Phi}. \tag{4}$$

The real quantity φ_c is the order parameter of the system, i.e., $\varphi_c^2 \sim n_c$, where n_c is the number density of particles in the condensate, and the real value Φ is a phase. In a fermionic system with pairing, the density n_c is proportional to the pairing gap Δ.

The equation for the electromagnetic field A_μ in such a system reads

$$\Box A_\mu = 4\pi j_\mu, \tag{5}$$

where the current is

$$j_\mu = ei\bar{\psi}\gamma_\mu\psi - ei(\varphi^*\partial_\mu\varphi - \varphi\partial_\mu\varphi^*) - 2e^2|\varphi|^2 A_\mu. \tag{6}$$

Substituting Eq. (4) into Eq. (6), we obtain for the electromagnetic current

$$j_\mu = j_\mu^A + \delta j_\mu, \tag{7}$$

where the first term $j_\mu^A = -2e^2\varphi_c^2 A_\mu$ is the superconducting current, and the second term δj_μ contains the normal current j_μ^{nor} and some response j_μ^{res} from the charged condensate, i.e.,

$$\delta j_\mu = j_\mu^{nor} + j_\mu^{res} = ei\bar{\psi}\gamma_\mu\psi + 2e\varphi_c^2\partial_\mu\Phi_0. \tag{8}$$

Due to gauge invariance, the phase $\Phi = \Phi_0 + \Phi'$ is not constrained, and Φ_0 can be chosen in such a way that it cancels the normal current, i.e., $\delta j_\mu = 0$; otherwise the remaining part of the normal current would destroy superconductivity and the ground state energy would increase. This compensation of the normal current j_μ^{nor}, which in metals and in normal plasma is proportional to the electric field $\mathbf{E}$, is a necessary condition for the existence of superconductivity. Only a diamagnetic part of the fermionic current proportional to the electromagnetic field A_μ may remain. The latter may lead only to a minor ($\sim e^2$) contribution

to the unit values of dielectric and diamagnetic constants. The remaining part of the phase Φ' is hidden in the gauge field, resulting in the disappearance of the Goldstone field (see the analogous discussion of the Higgs effect, e.g., in Ref. [22]). The total number of degrees of freedom does not change, so the disappearance of the Goldstone field is compensated by the appearance of an extra (third) polarization of the photon. As a result of Eqs. (5) and (7), the electromagnetic field obeys the equation

$$\Box A_\mu = -8\pi e^2 \varphi_c^2 A_\mu , \tag{9}$$

which immediately yields the photon spectrum in the form (3), where the photon mass is now given by

$$m_\gamma = \sqrt{8\pi e^2 \varphi_c^2}. \tag{10}$$

What we have demonstrated is known as the Higgs–Meissner effect: in the presence of a superconducting component, the photon acquires finite mass. We see that in a two-component (normal + superconducting) system, the photon is described by the dispersion relation (3), as it would be in a purely superconducting system, and not by a plasma-like dispersion law, as in the absence of superconductivity. Another way to arrive at Eq. (3) is given in the Appendix in a noncovariant formulation. Similar derivations for different specific physical systems, guided by the general principle of the compensation of the normal currents in a superconductor, can be found in Refs. [18, 20, 21, 23].

Expressing the amplitude of the condensate field in terms of the paired proton density [18], one obtains from Eq. (10) the result (2). Taking $m_p^*(\rho_0) \simeq 0.8 m_N$ (with m_N the free nucleon mass), with Eqs. (1) and (2) we estimate

$$m_\gamma(\rho = \rho_0, T) \text{ [MeV]} \simeq 1.6\sqrt{\frac{T_{c,p} - T}{T_{c,p}}} \ll \omega_{pl}(\rho \sim \rho_0).$$

Due to the rather low effective photon mass in superconducting neutron star matter at $T < T_{c,p} < \omega_{pl}$, one may expect a corresponding increase in the contribution of the above diagrams to neutrino emissivity.

To avoid misunderstanding, we note the following. At the first glance one might suggest that the photon self-energy is completely determined by the above neutrino production diagrams, but with neutrino legs replaced by a photon line. If so, the contributions of the electron-loop and proton-loop diagrams would accurately determine the plasmon spectrum of photon excitations with energy gap equal to a high plasma frequency (at least if one drops small terms proportional to the proton gap in the calculation of the proton–proton-hole diagram, now with an incoming and outgoing photon, as suggested for the corresponding neutrino process). How does this relate to the massive photon spectrum of superconducting systems? The answer is that in a system with a charged condensate, in addition to the cited photon propagation diagrams, there appear specific diagrams for photon rescattering off the condensate given by terms proportional to $e^2 \varphi_c^2 A_\mu A^\mu$ and $2e\varphi_c^2 \partial_\mu \Phi A^\mu$ in the corresponding Lagrangian. Their contributions to the equation of motion for the electromagnetic field are, respectively, the last two condensate terms in the electromagnetic current in Eq. (6). The specific condensate diagrams responsible for the compensation of the loop diagram contributions in the photon propagator make no contribution to neutrino emissivity. Indeed, the neutrino legs cannot be directly connected to the photon line via such interactions (without invoking the internal structure of the condensate order parameter

φ_c; this contribution is obviously small compared to what we have taken into account). Thus, we have argued that in the presence of superconducting protons, neutrino pairs can be produced in the reaction shown by the above diagrams, where the photons possess rather small masses generated by the Higgs–Meissner mechanism.

Having clarified of this important issue, we are ready to calculate the contribution of these processes to neutrino emissivity and compare the result with known emission rates.

3. CALCULATION OF EMISSIVITY

The matrix element of the above diagrams for the i-th neutrino species ($i = \{\nu_e, \nu_\mu, \nu_\tau\}$) is

$$\mathscr{M}^{(i)a} = -i\sqrt{4\pi}\, e \frac{G}{2\sqrt{2}} \varepsilon_\mu^a \left(\Gamma_\gamma T_p^{(i)\mu\rho} - T_e^{(i)\mu\rho}\right) l_\rho, \tag{11}$$

where

$$T_j^{(i)\mu\rho} = -\,\mathrm{Tr} \int \frac{d^4p}{(2\pi)^4} \gamma^\mu\, i\hat{G}_j(p)\, W_j^{(i)\rho}\, i\hat{G}_j(p+k), \quad j = \{e,p\}, \tag{12}$$

and

$$\hat{G}_j(p) = (\hat{p} + m_j) \left\{ \frac{1}{p^2 - m_j^2} + 2\pi\, i\, n_j(p)\, \delta(p^2 - m_j^2)\theta(p_0) \right\} \tag{13}$$

is the in-medium electron (proton) Green's function; $n_j(p) = \theta(p_{Fj} - p)$; ε_μ^a is the corresponding polarization four-vector of the massive photon, with three polarization states in superconducting matter. The factor Γ_γ takes into account nucleon–nucleon correlations in the photon vertex. The quantity $G = 1.17 \cdot 10^{-5}$ GeV^{-2} is the Fermi constant of the weak interaction. Above, l_ρ denotes the neutrino weak current. The electron and proton weak currents are

$$W_e^{(i)\rho} = \gamma^\rho (c_V^{(i)} - c_A^{(i)}\gamma_5), \qquad W_p^\rho = \gamma^\rho (\kappa_{pp} - g_A \gamma_{pp}\gamma_5), \tag{14}$$

where $c_V^{(\nu_e)} = c_V^{(+)} = 1 + 4\sin^2\vartheta_W \simeq 1.92$ and $c_V^{(\nu_\mu)} = c_V^{(\nu_\tau)} = c_V^{(-)} = 1 - 4\sin^2\vartheta_W \simeq 0.08$; ϑ_W is the Weinberg angle, and $c_A^{(\nu_e)} = -c_A^{(\nu_\mu,\nu_\tau)} = 1$. Proton coupling is corrected by nucleon–nucleon correlations, i.e., by the factors κ_{pp} and γ_{pp} [24].

Integrating Eq. (12) over the energy variable, we obtain for the i-th neutrino species

$$-\,i\left(T_p^{(i)\mu\rho} - T_e^{(i)\mu\rho}\right) = \tau_t^{(i)} P^{\mu\rho} + \tau_l^{(i)} F^{\mu\rho} + \tau_5^{(i)} P_5^{\mu\rho}, \tag{15}$$

$$P^{\mu\rho} = (g^{\mu\rho} - \frac{k^\mu k^\rho}{k^2} + F^{\mu\rho}), \quad F^{\mu\rho} = \frac{j^\mu j^\rho}{k^2[(k\cdot u)^2 - k^2]}, \quad P_5^{\mu\rho} = \frac{i}{\sqrt{k^2}} \varepsilon^{\mu\rho\delta\lambda} k_\delta u_\lambda, \tag{16}$$

where $j^\mu = (k\cdot u)k^\mu - u^\mu k^2$, $(k\cdot u) = k_\mu u^\mu$, $k^\mu = (\omega, \mathbf{k})$, $k^2 = k_\mu k^\mu = \omega^2 - \mathbf{k}^2$. The four-velocity u^μ of the medium is introduced for the sake of covariant notation. The transverse (τ_t), longitudinal (τ_l), and axial (τ_5) components of the tensors in Eq. (15) yield

$$\tau_t^{(i)} = \tau_{te}^{(i)} - \tau_{tp}^{(i)} = 2c_V^{(i)}(A_e + k^2 B_e) - 2c_V^{(-)} R_\kappa (A_p + k^2 B_p), \tag{17}$$

$$\tau_l^{(i)} = \tau_{le}^{(i)} - \tau_{lp}^{(i)} = 4k^2[c_V^{(i)}B_e - c_V^{(-)}R_\kappa B_p], \tag{18}$$

$$\tau_5^{(i)} = \tau_{5e}^{(i)} - \tau_{5p}^{(i)} = (k^2)^{3/2}[c_A^{(i)}C_e - g_A\gamma_{pp}C_p], \tag{19}$$

where $R_\kappa = \kappa_{pp}/c_V^{(-)}$, and

$$A_j = \int \frac{d^3p}{(2\pi)^3}\frac{n_j(p)}{E_p^{(j)}} + \frac{k^2}{2}\left(1 + \frac{k^2}{2m_j^2}\right)m_j C_j, \tag{20}$$

$$B_j = \int \frac{d^3p}{(2\pi)^3}\frac{n_j(p)}{2E_p^{(j)}}\frac{1 - (\mathbf{pk})^2/E_p^{(j)2}\mathbf{k}^2}{\left(\omega - \mathbf{pk}/E_p^{(j)}\right)^2 - k^4/4E_p^{(j)4}}, \tag{21}$$

$$C_j = \int \frac{d^3p}{(2\pi)^3}\, n_j(p)\frac{m_j}{E_p^{(j)3}}\left[\left(\omega - \frac{\mathbf{pk}}{E_p^j}\right)^2 - \frac{k^4}{4E_p^{(j)4}}\right]^{-1}, \quad E_p^{(j)} = \sqrt{m_j^2 + \mathbf{p}^2}. \tag{22}$$

Here we note that the contribution of the axial component τ_5 to the resulting neutrino emissivity is small ($\tau_5/\tau_t \sim m_\gamma^2\tau_5/\omega^2\tau_l \sim m_\gamma/m_N^*$ for protons and $\sim (m_\gamma m_e/p_{Fe}^2)\ln(p_{Fe}/m_e)$ for electrons), so that it will be omitted.

The squared matrix element (11) for a certain neutrino species, summed over the lepton spins and averaged over the three photon polarizations, can be cast in the form

$$\overline{\sum|\mathscr{M}^{(i)}|^2} = \frac{4}{3}\pi e^2 G^2\left[\tau_t^{(i)2}\left(2\omega_1\omega_2 + 2\frac{(\mathbf{kq}_1)(\mathbf{kq}_2)}{\mathbf{k}^2}\right) - \right.$$
$$\left. - \tau_l^{(i)2}\left(\omega_1\omega_2 + \mathbf{q}_1\mathbf{q}_2 - 2\frac{(k\cdot q_1)(k\cdot q_2)}{k^2} - 2\frac{(\mathbf{kq}_1)(\mathbf{kq}_2)}{\mathbf{k}^2}\right)\right], \tag{23}$$

where $(k\cdot q_{1,2}) = \omega\omega_{1,2} - (\mathbf{kq}_{1,2})$, and $\omega_{1,2}$ and $\mathbf{q}_{1,2}$ denote the frequencies and momenta of the neutrino and antineutrino. We have also used the fact that $\mathrm{Tr}\{l^\mu l^\nu\} = 8[q_1^\mu q_2^\nu + q_2^\mu q_1^\nu - g^{\mu\nu}(q_1\cdot q_2) - 4i\varepsilon^{\mu\nu\lambda\rho}q_{1\lambda}q_{2\rho}]$.

The emissivity of our processes is given by

$$\varepsilon_\nu^\gamma = \int \frac{d^3k}{(2\pi)^3 2\omega}\frac{d^3q_1}{(2\pi)^3 2\omega_1}\frac{d^3q_2}{(2\pi)^3 2\omega_2}\frac{\omega_1+\omega_2}{\exp[(\omega_1+\omega_2)/T]-1}\times$$
$$\times \sum_{i=\nu_e,\nu_\mu,\nu_\tau}\overline{\sum|\mathscr{M}^{(i)}|^2}(2\pi)^4\delta^4(k - q_1 - q_2). \tag{24}$$

Substituting Eq. (23) into Eq. (24), we finally obtain

$$\varepsilon_\nu^\gamma = \frac{T^5}{9(2\pi)^3}\pi e^2 G^2\alpha^2 I, \qquad I = \int_\alpha^\infty \frac{d\xi\,\xi}{e^\xi - 1}\sqrt{\xi^2 - \alpha^2}\left[\tau_t^2\left(\frac{\alpha^2}{\xi^2}\right) + \tau_l^2\left(\frac{\alpha^2}{\xi^2}\right)\right], \tag{25}$$

where $\alpha = m_\gamma/T$, and

$$\tau_t^2(x) \approx 4 \sum_{i=\nu_e,\nu_\mu,\nu_\tau} \left[c_V^{(-)} R_\kappa \frac{\rho_p}{2m_p^*}(1+x) - c_V^{(i)} \left(\frac{3}{8\pi}\rho_p\right)^{2/3} \left(1+\frac{x}{2}\right)\right]^2, \quad (26)$$

$$\tau_l^2(x) \approx 4x^2 \sum_{i=\nu_e,\nu_\mu,\nu_\tau} \left[c_V^{(-)} R_\kappa \frac{\rho_p}{2m_p^*} - c_V^{(i)} \left(\frac{3}{8\pi}\rho_p\right)^{2/3}\right]^2. \quad (27)$$

Some numerically small terms have been dropped in Eq. (26).

The integral I in Eq. (25) can be calculated analytically in the two limiting cases, $\alpha \ll 1$ and $\alpha \gg 1$:

$$I(\alpha \gg 1) \approx \frac{\sqrt{2\pi}}{2}\alpha^{3/2}\left(1+\frac{3}{2\alpha}\right) e^{-\alpha} \left[\tau_l^2(1) + \tau_t^2(1)\right], \quad (28)$$

$$I(\alpha \ll 1) \approx 2\zeta(3)\left[\tau_l(0) + \tau_t^2(0)\right], \quad \zeta(3) \simeq 1.202. \quad (29)$$

Thus, combining Eqs. (1) and (25)–(28), we obtain an estimate for emissivity of our reactions (we present here the result for $m_\gamma > T$ and for three neutrino species):

$$\varepsilon_\nu^\gamma \left[\frac{\text{erg}}{\text{cm}^3 \cdot \text{s}}\right] \approx 2.6 \cdot 10^{25} T_9^{3/2} \exp\left(-\frac{m_\gamma}{T}\right) \left(\frac{m_\gamma}{\text{MeV}}\right)^{7/2} \left(\frac{\rho}{\rho_0}\right)^{8/3} \left(1+\frac{3}{2}\frac{T}{m_\gamma}\right)[1+\eta], \quad (30)$$

$$\eta = 0.0003 R_\kappa^2 \left(\frac{m_p}{m_p^*}\right)^2 \left(\frac{\rho}{\rho_0}\right)^{4/3} - 0.035 R_\kappa \frac{m_p}{m_p^*}\left(\frac{\rho}{\rho_0}\right)^{2/3}. \quad (31)$$

Here T_9 denotes temperature measured in units of 10^9 K. The unity in square brackets in Eq. (30) corresponds to the electron–electron-hole diagram, whereas the factor η is related to the proton–proton-hole (first term in Eq. (31)) and the interference diagrams (second term in Eq. (31)).

Emissivity given by Eq. (30) varies with temperature as $T^{3/2}\exp(-m_\gamma/T)$, whereas emissivity of the modified URCA process varies as $T^8 \exp[-(\Delta_p+\Delta_n)/T]$ in the region of proton ($\Delta_p \neq 0$) and neutron ($\Delta_n \neq 0$) pairing. Hence, one can expect that the process $\gamma_m \to \nu\bar{\nu}$ will dominate at comparatively low temperatures, when $\Delta_p(T)+\Delta_n(T)-m_\gamma(T) > 0$ and $T < T_{c,p}$.

4. NUMERICAL ESTIMATES

To obtain quantitative estimates we need the values of the nucleon–nucleon correlation factors κ_{pp} and Γ_γ. According to Ref. [24], we can exploit

$$\kappa_{pp} = c_V^{(-)} - 2 f_{np} C_0 A_{nn} \Gamma(f_{nn}), \quad (32)$$

where $f_{np} \simeq -0.75$ and $f_{nn} \simeq 1.25$ are the constants in the theory of finite Fermi systems [19, 24]; $C_0^{-1} = m_n^* p_{Fn}/\pi^2$ is the density of states at the Fermi surface; A_{nn} is the neutron–neutron-hole loop,

$$C_0 A_{nn} = i C_0 \int \frac{d^3p}{(2\pi)^4} G_n(p+k) G_n(p) \approx \frac{p_{Fn}^2 k^2}{6 m_n^* \omega^2}, \quad (33)$$

for values of $\omega \gg |\mathbf{k}|p_{Fn}/m_n^*$ of interest, and $\Gamma^{-1}(f_{nn}) = 1 - 2f_{nn}C_0A_{nn}$.

We note that the second term in Eq. (32) is not proportional to a small factor $c_V^{(-)}$, because the nucleon–nucleon correlations also allow for emission of $\nu\bar{\nu}$-pairs from the nn^{-1} loop. Numerical estimates of the ratio R_κ are as follows: for $\alpha \gg 1$, we have $R_\kappa \simeq 1.6$ for $\rho = \rho_0$, $m_n^*(\rho_0) \simeq 0.8m_n$, and $R_\kappa \simeq 2.1$ for $\rho = 2\rho_0$, $m_n^*(2\rho_0) \simeq 0.7m_n$; for $\alpha \ll 1$, we obtain $R_\kappa \simeq 1$ and correlation effects are negligible. The in-medium renormalization of the proton electric charge included in the factor Γ_γ can be also expressed in terms of the constants in the theory of finite Fermi systems and the proton–proton loop factor (A_{pp}); see Ref. [19]. The latter is suppressed at relatively low proton densities. We can therefore take $\Gamma_\gamma \approx 1$. With these estimates, we observe that the main contribution to neutrino emissivity comes from electron–electron-hole processes.

The ratio of emissivity ε_ν^γ (30) to emissivity ε_ν^{FM} of the modified URCA process, $R_{FM} = \varepsilon_\nu^\gamma/\varepsilon_\nu^{FM}$, is

$$R_{FM} \approx 1.5 \cdot 10^4 T_9^{-13/2} \exp\left(\frac{\Delta_n + \Delta_p - m_\gamma}{T}\right)\left(\frac{m_\gamma}{\mathrm{MeV}}\right)^{7/2} \times$$
$$\times \left(1 + \frac{3}{2}\frac{T}{m_\gamma}\right)\left(\frac{\rho}{\rho_0}\right)^2 \frac{m_n^3 m_p}{m_n^{*3} m_p^*}[1 + \eta]. \qquad (34)$$

For further estimates we need the values of the neutron and proton gaps, which are unfortunately model-dependent. For instance, the evaluation in Ref. [25] yields $\Delta_n(0) \simeq 8.4T_{c,n} \simeq 0.6$ MeV, $T_{c,n} \simeq 0.07$ MeV for $3P_2$ neutron pairing at $\rho = \rho_0$, and $\Delta_p(0) \simeq 1.76T_{c,p} \simeq 3$ MeV, $T_{c,p} \simeq 1.7$ MeV for $1S$ proton pairing, while Ref. [26] uses $\Delta_n(0) \simeq 2.1$ MeV, $T_{c,n} \simeq 0.25$ MeV and $\Delta_p(0) \simeq 0.7$ MeV, $T_{c,p} \simeq 0.4$ MeV for $\rho = \rho_0$. Employing these estimates of the zero-temperature gaps, its temperature dependence, and the photon effective mass, we obtain from Eq. (34) the temperature dependence of the ratio R_{FM}.

In order to find the lower temperature limit at which the processes $\gamma_m \to \nu\bar{\nu}$ are still operative, we need to compare the value ε_ν^γ with photon emissivity at the neutron star surface, $\varepsilon_\gamma^s = 3\sigma T_s^4/R$, where σ is the Stefan–Boltzmann constant, T_s denotes the surface temperature of the star, and R is the star's radius. By employing a relation [27] between the surface and interior temperatures, we obtain for $R_\gamma = \varepsilon_\nu^\gamma/\varepsilon_\gamma^s$

$$R_\gamma \approx 1.2 \cdot 10^9 T_9^{-0.7} \exp\left(-\frac{m_\gamma}{T}\right)\left(\frac{m_\gamma}{\mathrm{MeV}}\right)^{7/2}\left(1 + \frac{3}{2}\frac{T}{m_\gamma}\right)\left(\frac{\bar{\rho}}{\rho_0}\right)^{8/3}[1 + \eta], \qquad (35)$$

where the star radius and mass are taken to be 10 km and $1.4M_\odot$, with $M_\odot$ the solar mass and $\bar{\rho}$ some averaged value of the density in the neutron star interior.

The ratios R_{FM} and R_γ are plotted as a function of the temperature in Figure for both of the foregoing parameter choices. We see that our new processes are operative in the temperature range $1 \cdot 10^9$ K $\lesssim T \lesssim 8 \cdot 10^9$ K for the parameter choice of Ref. [25], and $1 \cdot 10^9$ K $\lesssim T \lesssim 4 \cdot 10^9$ K for the parameters of Ref. [26]. As one observes in Figure, within these intervals the new cooling channel might exceed known cooling processes by up to a factor 10^6.

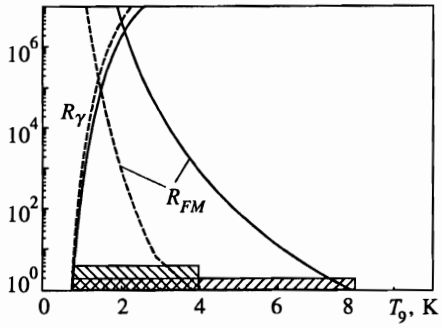

Temperature dependence of the ratios R_{FM} and R_γ at nucleon density $\rho = \rho_0$. Solid curves correspond to the parameter choice of Ref. [25], whereas the dashed curves depict results with parameters of Ref. [26]. Shaded bars indicate the temperature regions in which cooling via massive photon decay is more efficient than standard cooling processes

5. CONCLUDING REMARKS

As mentioned above, for $T > T_{c,n}, T_{c,p}$, i.e., in a normal plasma region of the star crust and star interior, photons with approximately the electron plasma frequency[1)] ω_{pl} can decay into neutrino pairs, as has been shown in previous estimates [10]. At $T < T_{c,p}$, however, we are already dealing with massive photons in the region of proton pairing, and our new reaction channels can significantly contribute to cooling.

Our processes can also occur in a charged-pion (or kaon) condensate state but they are suppressed due to the high effective photon mass[1)] $m_\gamma \simeq \sqrt{8\pi e^2 \varphi_c^2} \simeq 6$ MeV for the condensate field $\varphi_c \simeq 0.1 m_\pi \simeq 14$ MeV.

In deriving the value of ε_ν^{FM} used above, one describes the nucleon–nucleon interaction essentially by free one-pion exchange. In reality, however, at $\rho > (0.5\text{–}1)\rho_0$ the total nucleon–nucleon interaction does not reduce to free one-pion exchange, because of the strong polarization of the medium, whereby a significant part comes from in-medium pionic excitations [5–7, 24]. Occurring in intermediate states of the reaction, the in-medium pions can also decay into $e\bar{\nu}$, or first into a nucleon–nucleon-hole, which then radiates $e\bar{\nu}$, thereby substantially increasing the resulting emissivity. Other reaction channels such as $n \to n_{pair}\nu\bar{\nu}$ and $p \to p_{pair}\nu\bar{\nu}$ open up in the superfluid phase with paired nucleons [6, 24, 28], where n_{pair} (p_{pair}) means a paired neutron (proton). All these reaction channels give rise to a larger contribution to emissivity than that of the modified URCA process estimated via free one-pion exchange. Above we compared ε_ν^γ with ε_ν^{FM} just because the latter is used in the standard scenarios of neutron star cooling.

As we also mentioned in the Introduction, there are other processes like those considered above. Emissivity of the process $p\gamma_m \to p_{pair}\nu\bar{\nu}$ is substantially suppressed (at least by a factor e^2 and also due to a much smaller phase-space volume) compared to that of the process $p \to p_{pair}\nu\bar{\nu}$. According to simple estimates, e.g., using Eq. (22) of Ref. [16], the process $e\gamma \to e\nu\bar{\nu}$ makes a very small contribution to emissivity both in the inner crust and in the interior of neutron stars, even when one neglects the photon mass. Thus we may conclude that the process $e\gamma_m \to e\nu\bar{\nu}$ also leads to a minor contribution to emissivity at the densities and temperatures under consideration.

---

1) A rather small extra contribution also comes from the proton–proton-hole diagram.

1) For simplicity, in this estimate the peculiarities of a condensate with nonvanishing momentum [7] are ignored.

In summary, the processes $\gamma_m \to e e^{-1} + p p^{-1} \to \nu\bar{\nu}$ might be operative over some temperature interval $T \simeq 10^9$–10^{10} K, $T < T_{c,p}$, and together with other in-medium modified processes [8], they should be incorporated into computer simulations of neutron star cooling.

We acknowledge V. M. Osadchiev for fruitful discussions. The research described in this publication was made possible in part by Grants N3W000 from the International Science Foundation and N3W300 from the International Science Foundation and the Russian Government. B. K. and E. E. K. are supported by BMBF Grant 06DR666. E. E. K. acknowledges the support of the Heisenberg–Landau program.

APPENDIX

We can also achieve the same results that led to Eq. (10) by starting with Maxwell's equations (in obvious notation):

$$i\mathbf{kE} = 4\pi\tilde{\rho}, \quad i[\mathbf{kB}] = 4\pi\mathbf{j} - i\omega\mathbf{E},$$

$$\mathbf{kB} = 0, \quad [\mathbf{kE}] = \omega\mathbf{B},$$

where the charge density $\tilde{\rho}$ is the superposition of the density of free charges and the density of bound charge. Full free charge density being zero in our case due to local electroneutrality. The current $\mathbf{j}$ is a superposition of an external test current and the induced current:

$$\mathbf{j} = \mathbf{j}^{ext} + \mathbf{j}^{ind}.$$

In normal systems, the induced current (i.e., the current of nonpaired charged particles) $\mathbf{j}^{ind} = \mathbf{j}^{nor}$ is related to $\mathbf{E}$ via longitudinal ϵ_l and transverse ϵ_t dielectric constants. This connection results in longitudinal and transverse branches of the electromagnetic excitations, with an effective photon gap equal to the plasma frequency ω_{pl} [10]. In contrast, in a superconducting system the condensate makes two other contributions to the current, namely $\mathbf{j}^A = -2e^2\varphi_c^2\mathbf{A}$ and $\mathbf{j}^{res} = 2e\varphi_c^2\nabla\Phi$. Letting $\Phi = \Phi_{(1)} + \Phi_{(2)}$, we have $\mathbf{j}^{res} = \mathbf{j}^{res}_{(1)} + \mathbf{j}^{res}_{(2)}$. These two terms are determined as follows. As we have argued above, superconductivity requires the compensation of the normal component of the current proportional to $\mathbf{E}$, i.e., we can take $\mathbf{j}^{nor} + \mathbf{j}^{res}_{(1)} = 0$. Only small contributions $\sim e^2\exp(-\Delta_p/T)\omega^2\mathbf{A}$ and $\sim e^2\exp(-\Delta_p/T)\mathbf{k}^2\mathbf{A}$, as well as a small imaginary contribution $\sim ie^2F(\omega,\mathbf{k})\exp(-\Delta_p/T)\mathbf{A}$, where F is some function of ω and $\mathbf{k}$, can still remain from the value $\mathbf{j}^{nor}$ (see Eqs. (96.24) and (97.4) of Ref. [20]). We neglect these small contributions. The part of the current $\sim \nabla\Phi_{(2)}$ can be hidden in $\mathbf{j}^A$ by a gauge transformation of the field $\mathbf{A}$. We then have

$$i[\mathbf{kB}] \simeq \mathbf{j}^A - i\omega\mathbf{E}.$$

Taking the vector product of this equation with $\mathbf{k}$, we obtain

$$(\omega^2 - \mathbf{k}^2 - 8\pi e^2\varphi_c^2)\mathbf{B} = 0.$$

From this relation we observe that the electromagnetic excitations possess the mass given by Eq. (10). Hence, we have demonstrated that one can obtain the well-known plasma photon spectrum for a normal system, and at the same time one can obtain a massive photon spectrum and the Higgs–Meissner effect in a system with a charged condensate.

References

1. S. Shapiro and S. A. Teukolsky, *Black Holes, White Dwarfs and Neutron Stars: The Physics of Compact Objects*, Wiley, New York (1983), Ch. 1; *Neutron Stars*, ed. by D. Pines, R. Tamagaki, and S. Tsuruta, Addison-Weseley, New York (1992); H. Umeda, K. Nomoto, S. Tsuruta et al., Astrophys. J. **431**, 123 (1994); D. Page, E-print archive, astro-ph/9706259.
2. J. N. Bahcall and R. A. Wolf, Phys. Rev. B **140**, 1445 (1965); S. Tsuruta and A. G. W. Cameron, Can. J. Phys. **43**, 2056 (1965).
3. B. Friman and O. V. Maxwell, Astrophys. J. **232**, 541 (1979); O. V. Maxwell, Astrophys. J. **231**, 201 (1979).
4. S. Tsuruta, Phys. Rep. **56**, 237 (1979); K. Nomoto and S. Tsuruta, Astrophys. J. Lett. **250**, 19 (1981); Ch. Schaab, F. Weber, M. K. Weigel, and N. K. Glendenning, Nucl. Phys. A **605**, 531 (1996).
5. D. N. Voskresensky and A. V. Senatorov, Pis'ma Zh. Éksp. Teor. Fiz. **40**, 395 (1984) [JETP Lett. **40**, 1212 (1984)]; D. N. Voskresensky and A. V. Senatorov, Zh. Éksp. Teor. Fiz. **90**, 1505 (1986) [Sov. Phys. JETP **63**, 885 (1986)].
6. A. V. Senatorov and D. N. Voskresensky, Phys. Lett. B **184**, 119 (1987).
7. A. B. Migdal, E. E. Saperstein, M. A. Troitsky, and D. N. Voskresensky, Phys. Rep. **192**, 179 (1990).
8. Ch. Schaab, D. Voskresensky, A. D. Sedrakian, F. Weber, and M. K. Weigel, Astron. Astrophys. **321**, 591 (1997).
9. G. Flowers, P. G. Sutherland, and J. R. Bond, Phys. Rev. D **12**, 315 (1975).
10. J. B. Adams, M. A. Ruderman, and C.-H. Woo, Phys. Rev. **129**, 1383 (1963); D. A. Dicus, Phys. Rev. D **6**, 941 (1972); V. N. Oraevskii, V. B. Semikoz, and Ya. A. Smorodinsky, Part. and Nuclei **55**, 312 (1995); J. C. D'Olivio, J. F. Nieves, and P. Pal, Phys. Rev. D **40**, 3679 (1989).
11. M. Soyeur and G. E. Brown, Nucl. Phys. A **324**, 464 (1979).
12. B. Pontecorvo, Zh. Éksp. Teor. Fiz. **36**, 1615 (1959) [Sov. Phys. JETP **9**, 1148 (1959)].
13. G. G. Festa and M. A. Ruderman, Phys. Rev. **180**, 1227 (1969); D. A. Dicus, E. W. Kolb, D. N. Schramm, and D. L. Tubbs, Astrophys. J. **210**, 481 (1976).
14. H. J. Chiu and P. Morrison, Phys. Rev. Lett. **5**, 573 (1960); H. J. Chiu, Phys. Rev. **123**, 1040 (1961).
15. H. J. Chiu and R. C. Stabler, Phys. Rev. **122**, 1317 (1961).
16. V. I. Ritus, Zh. Éksp. Teor. Fiz. **41**, 1285 (1961) [Sov. Phys. JETP **14**, 915 (1962)].
17. V. Petrosian, G. Beaudet, and E. E. Salpeter, Phys. Rev. **154**, 1445 (1967); D. A. Dicus, Phys. Rev. D **6**, 941 (1972).
18. E. M. Lifshitz and L. P. Pitaevskii, *Statisticheskaya Fizika*, Chast' II, Nauka, Moskva (1978) [*Statistical Physics*, Part 2, Pergamon Press, New York (1980)].
19. A. B. Migdal, *Theory of Finite Systems and Properties of Atomic Nuclei* [in Russian], Nauka, Moscow (1983).
20. E. M. Lifshitz and L. P. Pitaevskii, *Fizicheskaya Kinetika*, Nauka, Moskva (1979) [*Physical Kinetics*, Pergamon Press, New York (1981)].
21. S. J. Putterman, *Superfluid Hydrodynamics*, North-Holland, Amsterdam, (1974); L. D. Landau and E. M. Lifshitz, *Gidrodinamika*, Nauka, Moskva (1986) [*Fluid Mechanics*, Pergamon Press, New York (1987)].
22. V. B. Berestetskii, *Problems of Elementary Particle Physics* [in Russian], Moscow, Nauka (1979).
23. B. J. Harrington and H. K. Shepard, Phys. Rev. D **19**, 1713 (1979); D. N. Voskresensky and N. Yu. Anisimov, Zh. Éksp. Teor. Fiz. **78**, 28 (1980) [Sov. Phys. JETP **51**, 13 (1980)]; D. N. Voskresensky, Zh. Éksp. Teor. Fiz. **105**, 1473 (1994) [Sov. Phys. JETP **78**, 793 (1994)].
24. D. N. Voskresensky and A. V. Senatorov, Yad. Fiz. **45**, 657 (1987) [Sov. J. Nucl. Phys. **45**, 411 (1987)].
25. T. Takatsuka, Prog. Theor. Phys. **48**, 1517 (1972).
26. D. Pines and M. A. Alpar, Nature **316**, 27 (1985).
27. E. H. Gudmundsson, C. J. Pethick, and R. I. Epstein, Astrophys. J. **272**, 286 (1983).
28. E. Flowers, M. Ruderman, and P. Sutherland, Astrophys. J. **205**, 541 (1976).